RSC Advances

PAPER

View Article Online
View Journal | View Issue

CrossMark click for updates

Cite this: *RSC Adv.*, 2017, **7**, 4704

Preparation of hydrophilic surface-imprinted ionic liquid polymer on multi-walled carbon nanotubes for the sensitive electrochemical determination of imidacloprid†

Lijuan Zhao, Juan Yang, Huili Ye, Faqiong Zhao* and Baizhao Zeng

A hydrophilic ionic liquid monomer (*i.e.* 1-(α-methyl acrylate)-3-vinylimidazolium bromide) was immobilized on carboxylated multi-walled carbon nanotubes (MWNTs) by ion exchange, then reversible addition–fragmentation chain transfer precipitation polymerization (RAFTPP) was performed in the presence of a template, imidacloprid. The obtained imidacloprid imprinted material showed a netlike structure; it had a large surface and high adsorption capacity, and allowed rapid mass transfer. When it was supported on a 1-(3-aminopropyl)-3-methylimidazolium bromide functionalized-graphene (GR-IL) coated glassy carbon electrode, the resulting sensor presented a good electrochemical response to imidacloprid. After optimizing the preparation and determination conditions, a linear range of 0.2–24 μM with a sensitivity of 0.71 μA μM^{-1} mm^{-2} was obtained. The detection limit was 0.08 μM. The sensor also presented good selectivity and reproducibility. It was successfully applied to the determination of imidacloprid in practical samples and the recovery for the standards added was 94–107%.

Received 28th October 2016
Accepted 29th November 2016

DOI: 10.1039/c6ra25969c

www.rsc.org/advances

Open Access Article. Published on 16 January 2017. Downloaded on 1/10/2025 8:53:25 AM.
This article is licensed under a Creative Commons Attribution 3.0 Unported Licence.

1. Introduction

Imidacloprid is an efficient pesticide and is widely used in agriculture. The pesticide generally acts as an antagonist by binding postsynaptic nicotinic receptors in the central nervous system of insects.[1,2] Its residue in agricultural products and the environment is harmful to human and animals,[3] thus its detection is required. So far, high performance liquid chromatography (HPLC),[4] gas chromatography-mass spectrometry (GC-MS),[5] liquid chromatography-mass spectrometry (LC-MS),[6] and electrochemical methods have been proposed for the determination of imidacloprid,[7–9] and electrochemical methods are thought to be quite suitable for it as it has good electroactivity. For example, a β-cyclodextrin polymer functionalized graphene modified electrode,[7] nanosilver-Nafion/nanoTiO_2-Nafion modified GCE[8] and molecularly imprinted poly(*o*-phenylendiamine)-graphene modified electrode[9] were constructed for the determination of imidacloprid. These electrodes had advantages of stability and easy preparation, but they had poor selectivity or low sensitivity.

Molecularly imprinted polymers (MIPs) are artificial-synthesized molecular recognition material.[10,11] As they show desired selectivity, physical robustness and thermal stability, they have been widely applied as sorbents and recognition elements.[12,13] MIPs are usually prepared through bulk polymerization, but the method usually results in incomplete template removal, small binding capacity and slow mass transfer rate.[14] To solve the problems, surface-imprinted techniques were proposed and become popular.[15,16] Recently, Gu *et al.*[17] prepared a molecularly imprinted core–shell structured poly(aniline-*co*-anthranilic acid) for the detection of dopamine, which showed high adsorption capacity and fast mass transfer rate; Zhang *et al.*[18] synthesized a molecularly imprinted poly(acrylamide) on multi-walled carbon nanotubes (MWNTs) for the electrochemical determination of parathion-methyl, and fast, selective and sensitive response was observed. Moreover, water-compatible MIPs should be synthesized to overcome the shortcoming that the recognition capacity of MIPs to strong hydrophilic target molecules is generally poor as using methacrylic acid (MAA) or 4-vinyl pyridine (4-VP) as functional monomer. Ionic liquids (ILs) have many unique characters such as non-volatility, non-flammability, high ion density and high ionic conductivity. As some IL monomers can interact with hydrophilic template molecules, IL-based water-compatible MIPs could be prepared.[19,20]

For the synthesis of MIP, free radical (FR) polymerization techniques are usually used due to their tolerance for a wide range of monomers and templates. However, the FR process does not allow control over the size, architecture and number of polymer molecules because of the chain-transfer and

Key Laboratory of Analytical Chemistry for Biology and Medicine (Ministry of Education), College of Chemistry and Molecular Sciences, Wuhan University, Wuhan 430072, Hubei Province, P. R. China. E-mail: fqzhao@whu.edu.cn; Fax: +86-27-68754067; Tel: +86-27-68752701

† Electronic supplementary information (ESI) available. See DOI: 10.1039/c6ra25969c

This journal is © The Royal Society of Chemistry 2017

Open Access Article. Published on 16 January 2017. Downloaded on 1/10/2025 8:53:25 AM.
This article is licensed under a Creative Commons Attribution 3.0 Unported Licence.

termination reactions.[21] To overcome these shortcomings controllable/"living" radical polymerization (CRP) methods can be introduced. Moreover, reversible addition–fragmentation chain transfer (RAFT) polymerization has been proven to be one of the most powerful CRP techniques because of its good control over the polymer structure, good applicability to different monomers and mild reaction conditions.[22–24] Owing to the presence of "living" fragments, RAFT polymerization has given access to hierarchical structures, core–shell materials and composites with tailor-made structures and improved properties. For examples, Gonzato *et al.*[21] used RAFT precipitation polymerization (RAFTPP) to prepare surface-imprinted Fe_3O_4 nanoparticles. Through this way Titirici *et al.*[25] obtained thin MIP film which combined covalent immobilization of azo initiator with RAFT polymerization on silica beads, and Pan *et al.*[26] prepared MIP particles with hydrophilic polymer brushes.

In this work, we presented a facile method for preparing hydrophilic surface-imprinted IL polymer. Firstly, hydrophilic IL monomer was introduced to the surface of carboxylated MWNTs through ion exchange, then RAFTPP was performed. Afterwards, the obtained composite material (MWNTs@RAFT-MIP) was immobilized on an IL functionalized graphene (GR-IL) modified electrode for imidacloprid sensing. As a result, the resulting electrochemical sensor exhibited high selectivity, sensitivity and fast response, and it was successfully applied to the detection of imidacloprid in practical samples.

2. Experimental

2.1 Reagents

Imidacloprid, dinotefuran, clothianidin and acetamiprid were purchased from Aladdin Chemistry Co., Ltd. (Shanghai, China) and their stock solutions (0.010 M) were prepared with ethanol and stored in a refrigerator at 4 °C. 2,2′-Azobis-(isobutyronitrile) (AIBN) was obtained from Shanghai Shisihewei Chemical Industry Limited Company (China) and used after twice recrystallization. 4-Vinylpyridine (4-VP) and ethylene glycol dimethacrylate (EGDMA) were purchased from Sigma-Aldrich (Madrid, Spain) and purified by distillation under vacuum. 1-Vinylimidazole and 2-(bromomethyl) acrylic acid came from J&K Chemical Ltd. (Shanghai, China). 2-Phenyl-2-propyl benzodithioate was from Sigma-Aldrich (Madrid, Spain). Ionic liquid 1-(α-methyl acrylate)-3-vinylimidazolium bromide (1-MA-3VI-Br) was synthesized in our laboratory and its structure was confirmed by ^{1}H NMR (see ESI†). The short multi-walled carbon nanotubes came from Xianfeng Reagent Co. Ltd. (Nanjing, China). Ionic liquid (1-(3-aminopropyl)-3-methylimidazolium bromide (IL-NH_2)) functionalized graphene (GR-IL) was synthesized as mentioned elsewhere.[27] All other chemicals used were of analytical reagent grade. The water used was redistilled.

2.2 Apparatus

Cyclic voltammetric and differential pulse voltammetric experiments were performed on a CHI 620D electrochemical workstation (CH Instrument Company, Shanghai, China). A conventional three-electrode system was adopted. The working electrode was a modified glassy carbon electrode (GCE, diameter: 2 mm), and the auxiliary and reference electrodes were a platinum wire and a saturated calomel electrode (SCE), respectively. The scanning electron microscope (SEM) images were obtained using field emission SEM (ZEISS, Germany). Ultraviolet visible (UV-Vis) absorption spectra were recorded by a U-3900 spectrometer (Hitachi Co., Japan). The Fourier transform infrared (FT-IR) absorption spectra were recorded with a model Nexus-670 spectrometer (Nicolet, USA). The pH values of solutions were measured with a pHS-2 meter (Leici Instrumental Factory, Shanghai, China). All experiments were carried out at room temperature.

2.3 Immobilization of hydrophilic IL monomer on MWNTs

At first, 400 mg purified MWNTs was dispersed in 300 mL concentrated nitric acid–sulfuric acid (1 : 3, v/v), heated to 70 °C and stirred for 120 min. After that, the reaction medium was diluted into 1000 mL and the MWNTs-COOH was collected by filtration and washed thoroughly with deionized water to neutrality. The filtered solid was dried in vacuum. Then 200 mL 0.5 M KOH aqueous solution was added. After sonicated for 5 h, the product was collected by filtration and washed with water, followed by dried at 60 °C under vacuum for 24 h. Thus MWNTs-COOK was obtained.

To immobilized IL monomer on MWNTs, 200 mg MWNTs-COOK and 0.7 mmol 1-MA-3VI-Br were added in 200 mL ethanol and let them react for 5 h at 50 °C. Then, the resulting product (*i.e.* MWNTs-IL) was filtered and washed thoroughly with water and ethanol for three times. Finally, it was dried at 70 °C under vacuum.

2.4 Preparation of hydrophilic surface-imprinted IL polymer

The hydrophilic surface-imprinted IL polymer was prepared *via* RAFTPP as shown in Scheme 1. Briefly, 25 mg imidacloprid (0.10 mmol) was added into a one-neck roundbottom flask (50 mL) with 25 mL methanol/water (4 : 1, v/v) solution, then

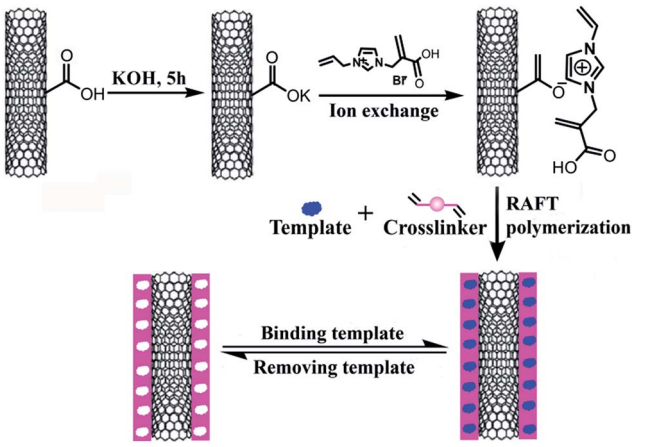

Scheme 1 Preparation of water-compatible surface-imprinted IL polymer coated MWNTs *via* RAFTPP.

Open Access Article. Published on 16 January 2017. Downloaded on 1/10/2025 8:53:25 AM.
This article is licensed under a Creative Commons Attribution 3.0 Unported Licence.

60 mg MWNTs-IL, 376 μL EGDMA (2.0 mmol), 21.3 μL 2-phenyl-2-propyl benzodithioate (0.088 mmol) and 7.2 mg AIBN (0.044 mmol) were added successively. After purged with argon for 15 min, the flask was sealed and immersed into a thermostatted oil bath at 60 °C for 24 h. The resulting gray polymer was collected by centrifugation and the template molecules were removed through Soxhlet extraction with methanol/acetic acid mixture (9 : 1, v/v, for about 48 h) and methanol (for about 24 h) until no template was detected in the extraction solution. After dried at 40 °C under vacuum to constant weight, gray MWNTs@RAFT-MIP was obtained. Similarly, non-imprinted polymer coated MWNTs (MWNTs@RAFT-NIP) was prepared and purified under the identical conditions except the absence of template.

For comparison, surface-imprinted IL polymer and non-imprinted polymer coated MWNTs (*i.e.* MWNTs@FR-MIP and MWNTs@FR-NIP) were also prepared by FRPP under the similar conditions but without 2-phenyl-2-propyl benzodithioate.

2.5 Preparation of sensors

The bare GCE was polished with slurry alumina (0.05 μm), and then washed thoroughly with water. Afterwards, 6.0 μL GR-IL suspension (1.0 mg mL^{-1} in water) was dropped on the cleaned GCE. After the solvent was evaporated under an infrared lamp, 5.0 μL MWNTs@RAFT-MIP suspension (2.0 mg mL^{-1} in DMF) was dropped onto the resulting GR-IL/GCE and let to dry in air. Thus an MWNTs@RAFT-MIP-GR-IL film coated GCE (*i.e.* MWNTs@RAFT-MIP-GR-IL/GCE) was obtained. For comparison, MWNTs@RAFT-NIP-GR-IL/GCE, MWNTs@FR-MIP-GR-IL/GCE and MWNTs@FR-NIP-GR-IL/GCE were prepared by a similar way.

2.6 Measurement of adsorption amount

The equilibrium adsorption amounts of the obtained MIP and NIP materials were determined as mentioned elsewhere.[28] The adsorption amount was calculated according to the formula: $Q = V(C_0 - C_S)/m$, where the symbols had normal physical meaning.

2.7 Electrochemical measurements

Certain imidacloprid stock solution and phosphate buffer solution (PBS, pH = 7.3) were transferred to a 10 mL cell, and the three-electrode system was installed on it. After accumulation for 6 min under open-circuit, cyclic voltammograms (CVs) or differential pulse voltammograms (DPVs) were recorded between −1.2 to −0.5 V. After each measurement, the electrode was rinsed with methanol–acetic acid solution (9 : 1, v/v) to remove imidacloprid for reuse.

3. Results and discussion

3.1 Preparation of hydrophilic surface-imprinted IL polymer

Previous research showed that ion exchange was an universal strategy to prepare IL functionalized MWNTs.[29,30] In this work, the IL monomer was immobilized on the surface of MWNTs *via* three-step. Firstly, the purified MWNTs were converted into MWNTs-COOH through the treatment of concentrated nitric acid–sulfuric acid solution; secondly, the MWNTs-COOH reacted with KOH solution to form MWNTs-COOK; thirdly, the IL monomer (*i.e.* IL-Br) was immobilized on MWNTs (MWNTs-IL) *via* ion exchange at 50 °C. The obtained MWNTs-IL (*i.e.* monomer) was hydrophilic, which could interact with template molecule imidacloprid through π–π stacking, hydrogen-bonding and electrostatic attraction. Afterwards, polymerization was performed with 2-phenyl-2-propyl benzodithioate as the chain transfer agent, while imidacloprid, MWNTs-IL, EGDMA, AIBN and methanol/water were utilized as the template, functional monomer, crosslinker, initiator and porogenic solvent, respectively. Thus, a water-compatible surface-imprinted IL polymer was obtained. As the support material MWNTs had large specific surface and high conductivity, and there was stronger interaction between monomer and template, the resulting molecularly imprinted material should have high adsorption capacity and be suitable for constructing electrochemical sensor for the determination of imidacloprid in aqueous solutions.

3.2 Morphological and structural characterization

As shown in Fig. 1, the crude MWNTs film presented network structure, and the average diameter of the MWNTs was about 25 nm. Like the MWNTs film, the MWNTs@RAFT-MIP film also displayed porous structure. The outer polymer shell on MWNTs was rough and nonuniform, and the average diameter of MWNTs@RAFT-MIP was about 40 nm, meaning that the thickness of the MIP layer was about 7.5 nm. As the composite film was netlike and the MIP layer was thin, the diffusion and adsorption of template molecules could be facilitated.

The FT-IR spectra of MWNTs-COOH, 1-MA-3VI-Br, MWNTs-IL and MWNTs@RAFT-MIP were recorded (Fig. S1†). The absorption peaks at 1723 cm^{-1} and 1624 cm^{-1} (curve a) should be ascribed to C=O and aromatic C=C stretching, which suggested that MWNTs-COOH was obtained. The 1-MA-3VI-Br exhibited a C=C stretching at 1640 cm^{-1}, and the characteristic vibration bands at 1563, 1459 and 1158 cm^{-1} (curve b) were assigned to the imidazolium cation, while the peaks at 2923 and

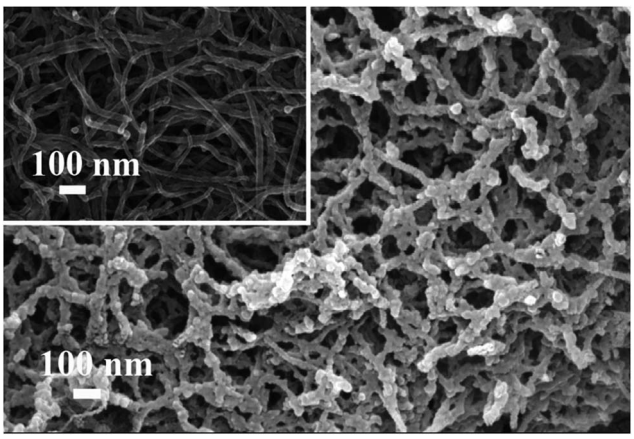

Fig. 1 SEM image of the MWNTs@RAFT-MIP. Inset: SEM image of MWNTs.

 This journal is © The Royal Society of Chemistry 2017

Open Access Article. Published on 16 January 2017. Downloaded on 1/10/2025 8:53:25 AM.
This article is licensed under a Creative Commons Attribution 3.0 Unported Licence.

2851 cm^{-1} were due to the asymmetric and symmetric CH_2 stretching. After the ion exchange, absorption bands corresponding to 1-MA-3VI-Br (curve c) appeared, indicating that MWNTs-IL was synthesized successfully. After imprinting polymerization *via* RAFTPP, the three main peaks around 1727 cm^{-1} (C=O stretching), 1257 and 1160 cm^{-1} (C–O–C stretching) proved the existence of poly(EGDMA), and the characteristic peaks corresponding to the aromatic C=C stretching (1624 cm^{-1}) of MWNTs could also be observed (curve d). In addition, the characteristic peaks of dithioester groups (*i.e.*, C=S stretching, around 1048 cm^{-1}) presented in the FT-IR spectra of MWNT@RAFT-MIP.

3.3 Adsorption amount

In order to investigate the binding performance of the MIP and NIP materials, an equilibrium binding analysis was carried out in the concentration range of 0.06–0.24 mM, and the adsorption curves of imidacloprid on the MIP and NIP materials were worked out (Fig. 2). As could be seen, compared with the MWNTs@FR-MIP, the MWNTs@RAFT-MIP showed higher binding capacity because of the intrinsic advantages of RAFTPP. When imidacloprid concentration exceeded 0.21 mM, the adsorption amounts of MWNTs@RAFT-MIP and MWNTs@FR-MIP kept almost unchanged, meaning that saturated adsorption was achieved. The maximum adsorption amounts of MWNTs@RAFT-MIP and MWNTs@FR-MIP were about 82 μmol g^{-1} and 76 μmol g^{-1}, respectively. For the MWNTs@RAFT-NIP, as it did not have specific recognition sites, its adsorption amount was smaller and it changed slowly with imidacloprid concentration increasing. Similarly, when imidacloprid concentration exceeded 0.15 mM, the adsorption curve of the MWNTs@RAFT-NIP exhibited a platform. The maximum adsorption amount was about 27.5 μmol g^{-1}. Obviously, through molecular imprinting, the adsorption amount of imidacloprid was greatly enhanced.

3.4 Voltammetric behavior of imidacloprid

Fig. 3 showed the CVs of imidacloprid at the MIP and NIP film modified electrodes. For the MWNTs@RAFT-MIP-GR-IL/GCE,

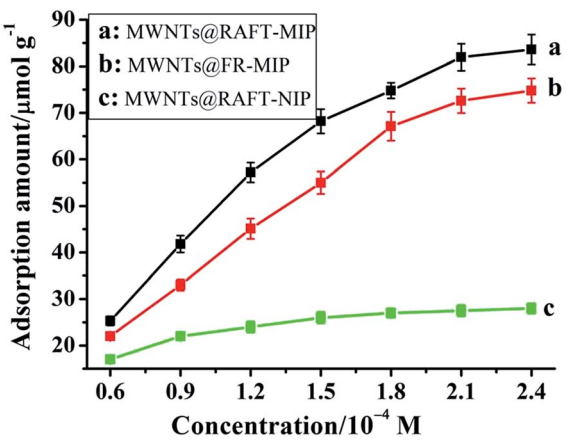

Fig. 2 Adsorption curves of imidacloprid on the MWNTs@RAFT-MIP (a), MWNTs@FR-MIP (b) and MWNTs@RAFT-NIP (c), respectively.

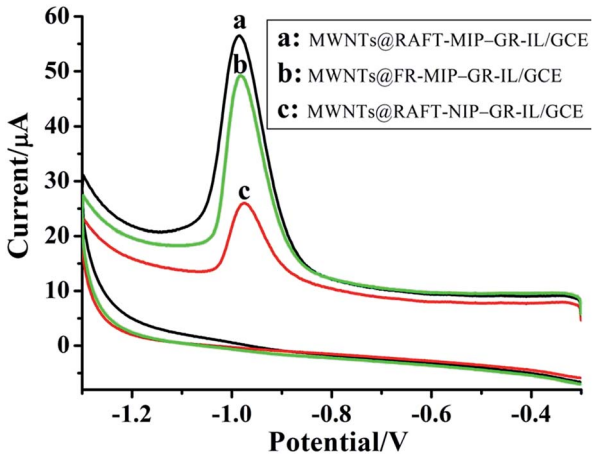

Fig. 3 Cyclic voltammograms of MWNTs@RAFT-MIP-GR-IL/GCE (a), MWNTs@FR-MIP-GR-IL/GCE (b) and MWNTs@RAFT-NIP-GR-IL/GCE (c) in PBS (pH 7.3) containing 50 μM imidacloprid. Scan rate: 50 mV s^{-1}.

imidacloprid exhibited a cathodic peak at about −0.92 V, corresponding to the irreversible reduction of nitro group to hydroxylamine group (Fig. S2†). The peak current of imidacloprid at the MWNTs@RAFT-MIP-GR-IL/GCE was higher than that at the MWNTs@FR-MIP-GR-IL/GCE, suggesting that the RAFTPP was more efficient. Although the same polymerization method was adopted, the obtained MWNTs@RAFT-NIP-GR-IL/GCE presented small response signal to imidacloprid, indicating that the MIP played key role in imidacloprid sensing.

3.5 Optimization of preparation and determination conditions

The influence of GR-IL amount on the voltammetric response of the resulting sensor was studied. As shown in Fig. S3A,† the peak current of imidacloprid reached a maximum when the volume of GR-IL suspension was up to 6.0 μL, then it decreased slowly. This was related to the variation of electrode surface area and electron transfer resistance. Therefore, 6.0 μL GR-IL suspension was adopted. It should pointed out, here GR-IL was selected as modifying material because it presented better performances than GR, MWNTs, *etc.*, in respect to stability and sensitivity.

The amount of MWNTs@RAFT-MIP was also varied to examine its influence (Fig. S3B†). It was found that the current response increased with the amount of MWNTs@RAFT-MIP rising due to the increase in the number of recognition sites. However, when the volume of MWNTs@RAFT-MIP suspension (2 mg mL^{-1}) exceeded 5.0 μL, the response signal gradually decreased because of the increase of transfer resistance. Thus, the volume of MWNTs@RAFT-MIP suspension was fixed at 5.0 μL.

As the electrochemical reaction of imidacloprid involves proton transfer, the solution pH does influence the peak current. Here the influence of solution pH was investigated in the range of 5.3–8.5 (Fig. S3C†). As could be seen, the peak current of imidacloprid increased with pH rising up to 7.3, and then it decreased with further increasing pH. Therefore, pH 7.3 phosphate buffer solution was selected as supporting

Open Access Article. Published on 16 January 2017. Downloaded on 1/10/2025 8:53:25 AM.
This article is licensed under a Creative Commons Attribution 3.0 Unported Licence.

electrolyte. At the same time, the peak potential (E_p) decreased linearly with increasing pH (Fig. 5C inset). A good linear relationship was obtained as follows: $E_p = -0.030\text{pH} - 0.710$. According to the Nernstian equation: $E \propto 59.16m/n$ pH (m: number of protons transferred; n: number of electrons transferred), we could see that the number of electron transferred was twice as the number of proton transferred in the electrochemical reaction.

The peak current also varied with accumulation time in the studied range (*i.e.* 2–8 min). As shown in Fig. S3D,† when it was above 6 min the peak current kept almost unchanged, meaning that saturated rebinding of imidacloprid on the MWNTs@RAFT-MIP-GR-IL/GCE was achieved. Therefore, 6 min was selected as the accumulation time for imidacloprid determination.

3.6 Calibration curve

Fig. 4 showed the DPVs of imidacloprid at the MWNTs@RAFT-MIP-GR-IL/GCE under the optimized experimental conditions. It could be seen that the peak current increased with increasing imidacloprid concentration. Furthermore, they presented good linear relationship over the range of 0.2–24 μM. The regression equation was I_P (μA) = 2.23c (μM) + 1.02 (R^2 = 0.995), with a sensitivity of 0.71 μA μM^{-1} mm^{-2}. The limit of detection was *ca.* 0.08 μM. Compared with some other modified electrodes, such as nanosilver-Nafion/nanoTiO$_2$-Nafion composite modified GCE,[8] molecularly imprinted poly(*o*-phenylendiamine)-graphene modified electrode,[9] β-cyclodextrin polymer functionalized graphene modified electrode,[31] poly(carbazole)/chemically reduced graphene oxide modified GCE[32] and activated GCE,[33] the MWNTs@RAFT-MIP-GR-IL/GCE showed a relatively wide linear range and a lower detection limit (Table S1†). Unlike MWNTs@RAFT-MIP-GR-IL/GCE, the MWNTs@RAFT-NIP-GR-IL/GCE showed a smaller linear range and lower sensitivity, which could be explained by the lack of specific binding sites on the surface of NIP film.

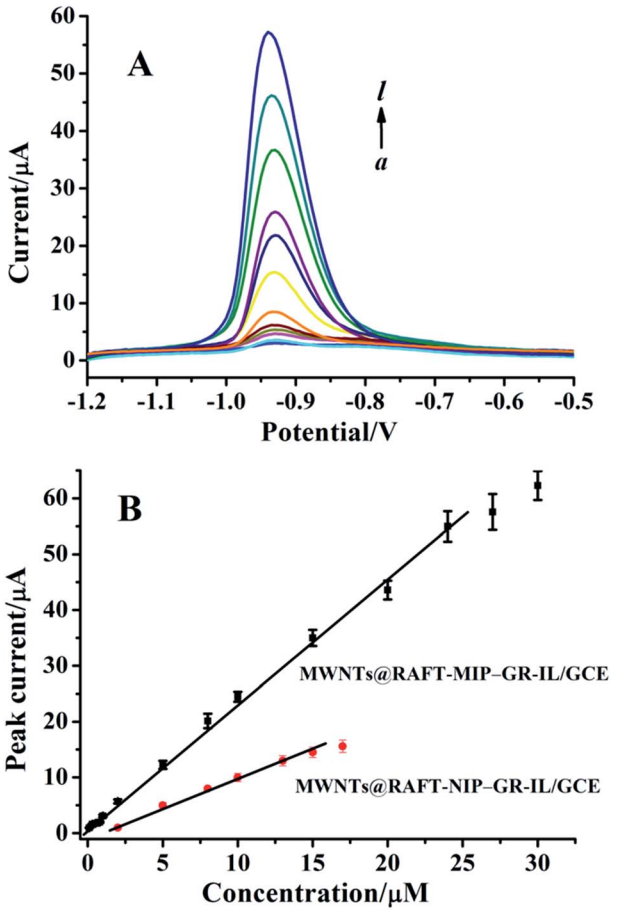

Fig. 4 (A) Differential pulse voltammograms of imidacloprid at MWNTs@RAFT-MIP-GR-IL/GCE. Imidacloprid concentration: 0.1, 0.5, 1.0, 2.0, 5.0, 8.0, 10, 13, 15, 17, 20, 24 μM (from a to l). (B) The calibration curves of imidacloprid at MWNTs@RAFT-MIP-GR-IL/GCE and MWNTs@RAFT-NIP-GR-IL/GCE.

3.7 Selectivity, repeatability and stability

The selectivity of the MWNTs@RAFT-MIP-GR-IL/GCE was evaluated by testing its electrochemical response to 5.0 μM imidacloprid in the presence of interfering substances, including dinotefuran, clothianidin, acetamiprid and *p*-nitrophenol. As shown in Fig. 5, in the presence of 10-fold interfering substances, the peak currents of imidacloprid displayed small change (from 95.4% to 107.8%), indicating that the MWNTs@RAFT-MIP-GR-IL/GCE had good selectivity.

To evaluate the reproducibility, five MWNTs@RAFT-MIP-GR-IL/GCEs were prepared by the same way and a 5.0 μM imidacloprid solution was determined. As a result, the relative standard deviation (RSD) of peak current was 5.6% (n = 5). The repeatability was investigated by monitoring a 5.0 μM imidacloprid solution using one sensor, and the RSD of peak current was 3.9% (n = 5). This indicated that the reproducibility of the MWNTs@RAFT-MIP-GR-IL/GCE was acceptable.

The stability was checked by storing the MWNTs@RAFT-MIP-GR-IL/GCE in a refrigerator at 4 °C for 7 days and tested its electrochemical response to 5.0 μM imidacloprid. The peak current well retained 92% of its initial value, and still retained

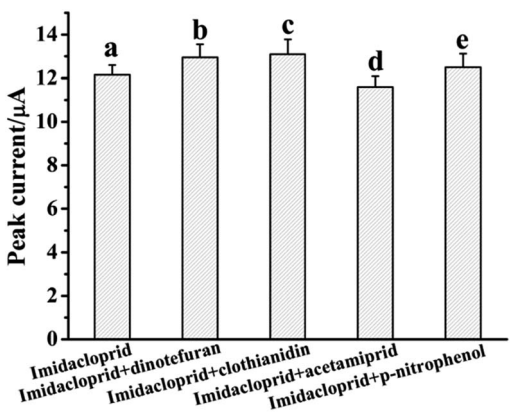

Fig. 5 Influence of coexistent substance on the electrochemical response of MWNTs@RAFT-MIP-GR-IL/GCE to imidacloprid. Solution composition: 5.0 μM imidacloprid, 5.0 μM imidacloprid plus 50 μM dinotefuran, 5.0 μM imidacloprid plus 50 μM clothianidin, 5.0 μM imidacloprid plus 50 μM acetamiprid, 5.0 μM imidacloprid plus 50 μM *p*-nitrophenol.

 This journal is © The Royal Society of Chemistry 2017

Open Access Article. Published on 16 January 2017. Downloaded on 1/10/2025 8:53:25 AM.
This article is licensed under a Creative Commons Attribution 3.0 Unported Licence.

Table 1 Determination results of imidacloprid in practical samples using a MWNTs@RAFT-MIP-GR-IL/GCE

Sample	Imidacloprid added (μM)	Imidacloprid found (μM)	Recovery (%)	RSD (%) ($n = 5$)
Cabbage	0	—	—	—
	0.50	0.54	108	5.2
	2.00	2.04	102	3.9
	5.00	4.93	98.6	4.3
Apple peel	0	—	—	—
	0.50	0.47	94	3.7
	2.00	2.07	103.5	4.6
	5.00	5.35	107	2.9

86% after one month-store. These reflected the good stability of MWNTs@RAFT-MIP-GR-IL/GCE.

3.8 Application

In order to test its application feasibility, the electrochemical sensor was applied to the detection of imidacloprid in practical samples, including cabbage and apple peel. Prior to determination, they were grinded to slurry and then centrifuged, and 5.0 mL of the supernatant was weighed and diluted to 50 mL with 0.2 M PBS (pH = 7.3) for determination. But no imidacloprid was detected in these samples. Then standard solution was added and the recovery was estimated. The results were summarized in Table 1, the recovery was 94–107% for different samples and different concentration levels.

4. Conclusions

A RAFTPP approach was developed for preparing water-compatible imidacloprid imprinted IL polymer, in which IL monomer was immobilized on MWNTs. The obtained composite material combined the advantages of nanomaterial and surface-imprinting, and showed netlike structure, high adsorption capacity and fast mass transfer rate. When it was applied to constructing electrochemical imidacloprid sensor, good selectivity and high sensitivity were achieved.

Acknowledgements

The authors appreciate the financial support of the National Natural Science Foundation of China (Grant No. 21277105).

References

1 E. Giannakopoulos, P. Stivaktakis and Y. Deligiannakis, *Langmuir*, 2008, **24**, 3955–3959.
2 S. K. Papiernik, W. C. Koskinen, L. Cox, P. J. Rice, S. A. Clay, N. R. Werdin-Pfisterer and K. A. Norberg, *J. Agric. Food Chem.*, 2006, **54**, 8163–8170.
3 G. Liu and Y. Lin, *Electrochem. Commun.*, 2005, **7**, 339–343.
4 H. Liu, J. Song, S. Zhang, L. Qu, Y. Zhao, Y. Wu and H. Liu, *Pest Manage. Sci.*, 2005, **61**, 511–514.
5 A.-Y. Ko, M. M. Rahman, A. M. Abd El-Aty, J. Jang, J.-H. Park, S.-K. Cho and J.-H. Shim, *Food Chem.*, 2014, **148**, 402–409.
6 J. M. Bonmatin, I. Moineau, R. Charvet, C. Fleche, M. E. Colin and E. R. Bengsch, *Anal. Chem.*, 2003, **75**, 2027–2033.
7 M. Chen, Y. Meng, W. Zhang, J. Zhou, J. Xie and G. Diao, *Electrochim. Acta*, 2013, **108**, 1–9.
8 A. Kumaravel and M. Chandrasekaran, *Sens. Actuators, B*, 2011, **158**, 319–326.
9 L. Kong, X. Jiang, Y. Zeng, T. Zhou and G. Shi, *Sens. Actuators, B*, 2013, **185**, 424–431.
10 X.-A. Ton, B. Tse Sum Bui, M. Resmini, P. Bonomi, I. Dika, O. Soppera and K. Haupt, *Angew. Chem., Int. Ed.*, 2013, **52**, 8317–8321.
11 J. Orozco, A. Cortés, G. Cheng, S. Sattayasamitsathit, W. Gao, X. Feng, Y. Shen and J. Wang, *J. Am. Chem. Soc.*, 2013, **135**, 5336–5339.
12 A. Yarman and F. W. Scheller, *Angew. Chem., Int. Ed.*, 2013, **52**, 11521–11525.
13 T. Qian, C. Yu, X. Zhou, P. Ma, S. Wu, L. Xu and J. Shen, *Biosens. Bioelectron.*, 2014, **58**, 237–241.
14 G. Fu, H. He, Z. Chai, H. Chen, J. Kong, Y. Wang and Y. Jiang, *Anal. Chem.*, 2011, **83**, 1431–1436.
15 Y. Li, Q. Bin, Z. Lin, Y. Chen, H. Yang, Z. Cai and G. Chen, *Chem. Commun.*, 2015, **51**, 202–205.
16 L. Chang, Y. Ding and X. Li, *Biosens. Bioelectron.*, 2013, **50**, 106–110.
17 L. Gu, X. Jiang, Y. Liang, T. Zhou and G. Shi, *Analyst*, 2013, **138**, 5461–5469.
18 D. Zhang, D. Yu, W. Zhao, Q. Yang, H. Kajiura, Y. Li, T. Zhou and G. Shi, *Analyst*, 2012, **137**, 2629–2636.
19 L. Chen, S. Xu and J. Li, *Chem. Soc. Rev.*, 2011, **40**, 2922–2942.
20 X. Luo, Y. Zhan, X. Tu, Y. Huang, S. Luo and L. Yan, *J. Chromatogr. A*, 2011, **1218**, 1115–1121.
21 C. Gonzato, M. Courty, P. Pasetto and K. Haupt, *Adv. Funct. Mater.*, 2011, **21**, 3947–3953.
22 S. Xu, J. Li and L. Chen, *J. Mater. Chem.*, 2011, **21**, 4346–4351.
23 Y. Ma, G. Pan, Y. Zhang, X. Guo and H. Zhang, *Angew. Chem., Int. Ed.*, 2013, **52**, 1511–1514.
24 M. Zhao, C. Zhang, Y. Zhang, X. Guo, H. Yan and H. Zhang, *Chem. Commun.*, 2014, **50**, 2208–2210.
25 M.-M. Titirici and B. Sellergren, *Chem. Mater.*, 2006, **18**, 1773–1779.
26 G. Pan, Y. Zhang, Y. Ma, C. Li and H. Zhang, *Angew. Chem., Int. Ed.*, 2011, **50**, 11731–11734.
27 L. Zhao, F. Zhao and B. Zeng, *Electrochim. Acta*, 2014, **115**, 247–254.
28 L. Zhao, F. Zhao and B. Zeng, *Biosens. Bioelectron.*, 2014, **60**, 71–76.
29 C. Fu, L. Meng, Q. Lu, Z. Fei and P. J. Dyson, *Adv. Funct. Mater.*, 2008, **18**, 857–864.
30 L. Meng, L. Niu, L. Li, Q. Lu, Z. Fei and P. J. Dyson, *Chem.–Eur. J.*, 2012, **18**, 13314–13319.
31 M. Chen, J. Wang, W. Zhang and G. Diao, *J. Electroanal. Chem.*, 2013, **696**, 1–8.
32 W. Lei, Q. Wu, W. Si, Z. Gu, Y. Zhang, J. Deng and Q. Hao, *Sens. Actuators, B*, 2013, **183**, 102–109.
33 W. Si, Z. Han, W. Lei, Q. Wu, Y. Zhang, M. Xia and Q. Hao, *J. Electrochem. Soc.*, 2013, **161**, B9–B13.